IEEE Photonics Journal
An IEEE Photonics Society Publication

Open Access

High-Order-Tilted Fiber Bragg Gratings With Superposed Refractive Index Modulation

Volume 10, Number 1, February 2018

Xuan-Yu Zhang
Chao Chen
Yong-Sen Yu
Wei-Hua Wei
Qi Guo
Yong-Yi Chen
Xing Zhang
Li Qin
Yong-Qiang Ning
Hong-Bo Sun, *Fellow, IEEE*

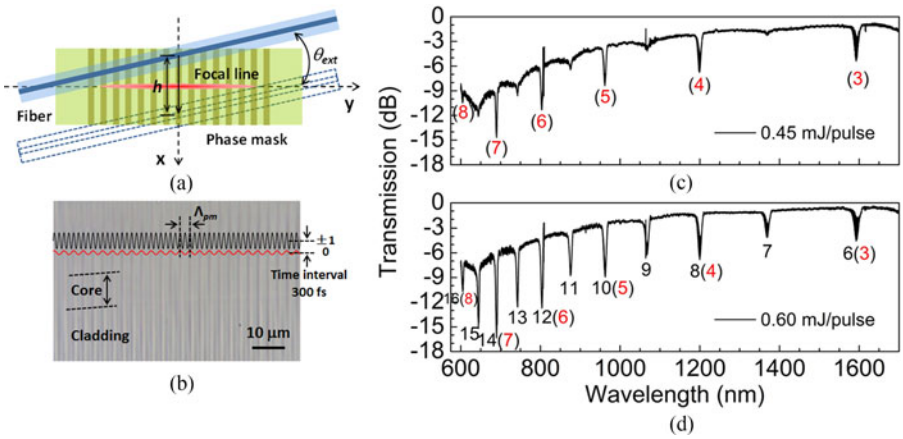

DOI: 10.1109/JPHOT.2017.2784818

IEEE photonics SOCIETY
IEEE

High-Order-Tilted Fiber Bragg Gratings With Superposed Refractive Index Modulation

Xuan-Yu Zhang,[1] Chao Chen,[2] Yong-Sen Yu,[1] Wei-Hua Wei,[1] Qi Guo,[1] Yong-Yi Chen,[2] Xing Zhang,[2] Li Qin,[2] Yong-Qiang Ning,[2] and Hong-Bo Sun,[1,3] *Fellow, IEEE*

[1]State Key Laboratory on Integrated Optoelectronics, College of Electronic Science and Engineering, Jilin University, Changchun 130012, China
[2]State Key Laboratory of Luminescence and Application, Changchun Institute of Optics, Fine Mechanics and Physics, Chinese Academy of Sciences, Changchun 130033, China
[3]State Key Laboratory of Precision Measurement and Instruments, Department of Precision Instrument, Tsinghua University, Beijing 100084, China

DOI:10.1109/JPHOT.2017.2784818

Manuscript received October 22, 2017; revised November 28, 2017; accepted December 12, 2017. Date of publication December 19, 2017; date of current version January 4, 2018. This work was supported in part by the National Natural Science Foundation of China under Grants 61505206, 61590930, 61234004, 61376070, and 61405190, in part by the Science and Technology Development Project of Jilin Province under Grant 20150520089JH, and in part by the National Science and Technology Major Project of China under Grant 2016YFE0126800. X.-Y. Zhang and C. Chen contributed equally to this work. Corresponding authors: Y.-S. Yu (yuys@jlu.edu.cn).

Abstract: A high-order-tilted fiber Bragg gratings (HO-TFBG) with superposed refractive index (RI) modulation written by a femtosecond laser and a phase mask has been demonstrated. The superposed grating structure is realized by the combined action of the pure ± 1 order pulses interference and the heat accumulation effect of ± 1 order and zero-order pulses. For the phase mask with the pitch of 3.33 μm, there are 11 groups of high-order Bragg resonance and cladding mode resonances sets in the wavelength range of 600–1700 nm, the information carried by which is doubled compared to the HO-TFBG written by pure two beams interference. It demonstrates that the sensitivities of the cladding mode resonances sets to surrounding RI, axial strain and temperature decrease with the increase of the grating order.

Index Terms: Fiber Bragg gratings (FBG), fiber optics sensors, femtosecond (fs) laser, laser materials processing.

1. Introduction

Tilted fiber Bragg gratings (TFBGs) have Bragg resonance and cladding mode resonances in their characteristic spectra due to the grating wave vector direction deviates from the fiber axial direction [1]–[3]. Taking advantage of the different response characteristics of Bragg resonance and cladding mode resonances to surrounding perturbations, the TFBG has been used in the biochemical sensing area for refractive index (RI), humidity, concentration and cell detecting [3]–[6], as well as the physical sensing area for temperature, strain, bending and magnetic field measurement [2], [3], [7], [8]. As for the TFBG written by UV excimer laser, we usually consider that it has the sine RI distribution, the characteristic spectrum of which usually only contains the first order Bragg

resonance and the corresponding comb-like cladding mode resonances [2], [3]. For the special application area, such as the wavelength-division multiplexing, the single UV-written TFBG that contains only one waveband resonance is hard to fulfill the demands. It usually needs to cascade several TFBGs with different or same tilt angles to form resonances in much more wavebands and to increase the information and functionality carried by the sensor [9], [10]. For example, Baiad *et al.* proposed an inline multichannel surface plasmon resonance (SPR) sensor, which was constituted by cascading three TFBGs with the tilting angles of 4.5°, 6° and 4°, and multiplexing was realized based on the different operation wavelengths and polarization characteristics of each TFBG [9]; Feng *et al*. proposed a 3D shape sensor based on a pair of orthogonal 2° TFBGs, the measurements of magnitude and direction of curvature were realized with the different responses to curvature of two groups of cladding mode resonances, and the discrimination to strain was also realized with the Bragg wavelength shift [10]. However, the studies above increased not only the complexity of the structure, but also the difficulty and cost of the fabrication. The length of the sensor even reached 90 mm [9], which limited the possibility of the TFBGs to be used as a compact detector. Although we can increase the laser exposure dose substantially during the UV laser writing process of the FBG to make the RI distribution deviate sine function [11], due to the limitation of the saturated effect of the RI modulation, only the low order Fournier items are contained in the Fournier series of the RI modulation function, such as the resonances from 1st to 3rd order, and the resonance strength is weak [11]–[13].

Fortunately, the high-order TFBG (HO-TFBG) written by femtosecond (fs) laser provides the possibility of mitigating the problems mentioned above. The non-sine RI modulation ($\triangle n_{\text{mod}}$) of fs-written Bragg grating could provide the large enough high-order Fourier coefficients, which could be used to control the resonance strength [14]–[16]. In our previous work, the possibility of realizing HO-TFBG was demonstrated with pure two beams ($\pm$1 order diffraction beams) interference [17]. A single device showed the 3rd order and 4th order Bragg resonance and cladding mode resonances sets around 1200 nm and 1600 nm, respectively. In practical applications, we hope to present the denser high-order resonances in limited spectrum range, i.e., carrying more information, which is of great benefit to sensing functionality improvement. In the reported works, harmonics of the Bragg wavelength could be generated with the Talbot effect or multi-order diffractive beams interference of UV laser [12], [13], [18], [19], however, it was difficult for fs laser with the coherent length of 30 μm (pulse duration of 100 fs). Grobnic *et al.* increased the pulse duration with technique of chirping the Fourier transform limited fs pulse, the multi-beam interference of multi-diffraction order long length superposition was formed near the phase mask (the distance between fiber and phase mask was 500 μm), and fabricated composite grating with high density Bragg resonances [20], [21]. However, the complex laser pulse modulation was required, and it was difficult to control the grating spectrum by increasing the laser pulse energy due to the limitation of the damage threshold of phase mask.

Therefore, a HO-TFBG with superposed RI modulation written by fs laser and high-order phase mask is reported in this paper. The superposed grating structure is realized by taking advantage of the $\pm$1 order diffractive pulses interference combined with the heat accumulation effect of $\pm$1 order and zero order pulses, which act on the single mode fiber together in the diffractive order walk-off area. The characteristic spectrum of the fs-written HO-TFBG contains two kinds of high-order Bragg resonance and cladding mode resonances sets. Its distribution density is doubled compared with the TFBG written by pure two beams interference in the wide spectral range of 600–1700 nm. These two kinds of characteristic spectra correspond to the fringe periods of $\pm$1 order pulses interference light field and zero order light field, respectively. The three groups of cladding mode resonances sets above the cut-off wavelength are chosen and used to demonstrate the sensing characteristics of the sensor to surrounding RI, axial strain and temperature.

2. Experimental Details

The schematic diagram for fabricating the HO-TFBG is shown in Fig. 1, a Ti: Sapphire regenerative amplifier system is used to generate the fs pulse with the operation wavelength of $\lambda_{in} = 800$ nm, pulse duration of 100 fs and repetition rate of 100 Hz. The laser is focused in Corning SMF-

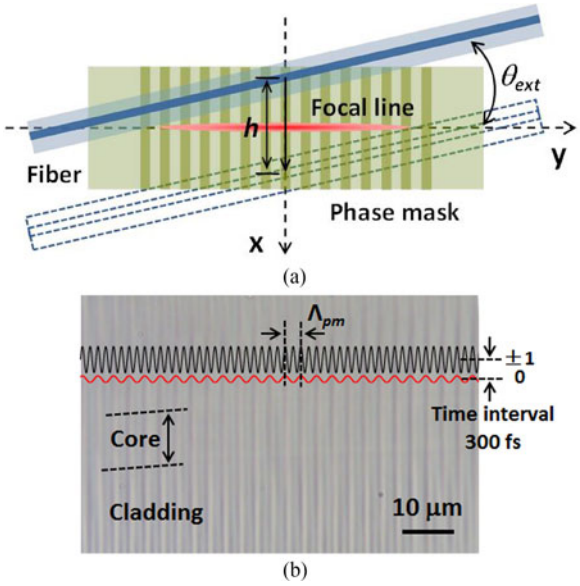

Fig. 1. (a) Schematic diagram of the setup for fabricating HO-TFBG. (b) Microscope image of the RI modulation pattern induced by fs laser, the presented 300 fs illustrates the time difference between zero order and ±1 order diffraction beams when transmitting to the fiber.

28e single mode fiber after passing through the cylindrical lens with focal length $f = 40$ mm and high-order phase mask (pitch, $\Lambda_{pm} = 3.33$ μm) with the zero order diffraction efficiency of 3%. For the beam radius with $\omega_0 = 2.5$ mm, the focal spot size is less than the fiber core diameter, due to the focal spot $\omega = \lambda_{in} f/\pi\omega_0 \approx 4$ μm. It is difficult to form effective interference fringe by tilting the phase mask, even if the angle is smaller than 1 degree. Therefore, the fabrication of the TFBG is realized with scanning exposing by tilting the fiber with the angle θ_{ext} and scanning along X axis with speed of 1 μm/s. The scanning range is determined by $h = 2\omega_0 \tan(\theta_{\text{ext}})$. According to the study by Mihailov *et al.*, the tilted angle of grating plane in the fiber can be determined by $\theta_{int} = \pi/2 - \arctan\left(n_{IR} \tan\theta_{\text{ext}}\right)^{-1}$ [22], in which, n_{IR} is the fiber core effective refractive index at 800 nm. In order to avoid damaging the silica phase mask by the high pulse energy, the phase mask is placed 3.0 mm away from the beam focus (i.e., the interval d between fiber and phase mask) to make the light intensity on the phase mask minimum. At the same time, this interval also satisfies the interference condition of pure ±1 order diffractive beams, i.e., $\cos\theta_{\pm1} L/(1 - \cos\theta_{\pm1}) < d < \omega_0/\tan\theta_{\pm1}$, in which, $\theta_{\pm1}$ is the ±1 order diffractive angle and L is the coherent length of fs pulse [23], [24]. The grating structure with the period of $\Lambda_{pm}/2$ will be formed as demonstrated in the existing studies. However, here we take advantage of the heat accumulation effect in the interacting process between the high repetition rate pulse and transparent materials [25]–[28]. The HO-TFBG with superposed RI modulation is realized by modulating the laser pulse energy, this device has the resonance spectrum characteristic with high density distribution.

The specific grating formation mechanism can be described as follows: when the fs pulse is diffracted by the phase mask, the group speed of each diffractive order pulse will be mismatched in the normal projection of the phase mask [23], [24]. As for the experiment condition in this paper, the zero and ±1 order diffractive pulses (defined as "twin pulses"), which come from the same fs pulse, will act on the fiber with the time interval of 300 fs successively. The frequency that the "twin pulses" expose the fiber is determined by the repetition rate of the fs laser. Since the energy carried by the zero order diffractive pulse is low (usually lower than the threshold of the RI change), it is difficult to induce RI modulation by the zero order diffractive pulse alone. However, in the time scale less than the lattice heat diffusion time (time scale of ps), before the earlier absorbed photon energy of zero order pulse is diffused by the electron-phonon scattering, the ±1 order pulse energy has already been absorbed. Therefore, the effects of these two kinds of pulses on fiber are not independent, the

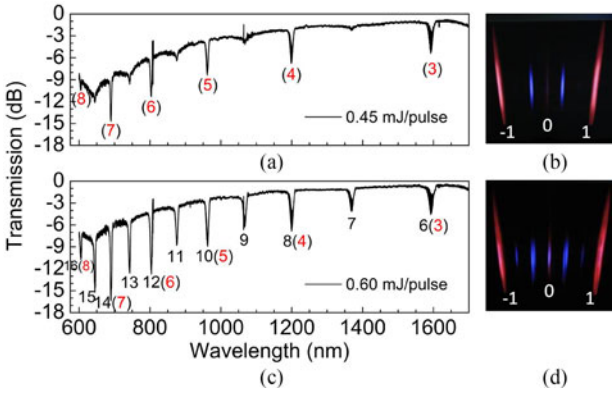

Fig. 2. The characteristic spectra of the HO-TFBGs written with the pulse energy of (a) 0.45 mJ/pulse and (c) 0.60 mJ/pulse. The diffractive light spot patterns achieved after the phase mask corresponding to (b) 0.45 mJ/pulse and (d) 0.60 mJ/pulse.

heat produced by the pulses will accumulate [25]–[27]. The phenomenon of RI change induced by "twin pulses" is similar to the interaction between high repetition rate pulse and material [25], [26]. Finally, the interference between ± 1 order pulses will induce the major grating, the period of which is 1.665 μm. The heat accumulation between ± 1 order and zero order pulses will induce additional grating on the major grating, the period of which is 3.33 μm. In this case, the incidence fs pulse energy needs to be higher than a critical value, for the experiment condition here, the critical pulse energy is about 0.5 mJ/pulse. The RI modulation pattern of the 3° TFBG is given in Fig. 1(b), it is realized with the fs laser pulse energy of 0.60 mJ/pulse and the scanning exposure time of about 260 secs. As can be seen, the additional grating is superposed on the major grating. Please notice that the RI change induced in the cladding, due to self-focusing effect of fs laser, will suppress the amplitude of cladding mode resonances [14], [29]. This problem could be solved by loading hydrogen in fiber or utilizing the cylindrical lens with short Rayleigh length to limit the RI change in the core of the fiber [30].

As can be expected, the high-order spectrum generated by these two kinds of periodical structures will appear simultaneously in wide spectral range according to the phase matching conditions of TFBG [1]–[3]. The phase matching conditions are as follows

$$m\lambda_{B,m} = 2n_{eff}^{\text{core}}\left(\lambda_{B,m}\right)\Lambda_g \tag{1}$$

$$m\lambda_{\text{clad},m}^{\nu\mu} = \left(n_{eff}^{\text{core}}\left(\lambda_{\text{clad},m}^{\nu\mu}\right) + n_{eff}^{clad}\left(\lambda_{\text{clad},m}^{\nu\mu}\right)\right)\Lambda_g \tag{2}$$

where m is the Bragg diffractive order number, Λ_g is the fiber axial projection of the grating period, $n_{eff}^{\text{core}}(\lambda_{B,m})$ is the effective RI of the core mode at the Bragg resonant wavelength $\lambda_{B,m}$, $n_{eff}^{\text{core}}(\lambda_{\text{clad},m}^{\nu\mu})$ and $n_{eff}^{clad}(\lambda_{\text{clad},m}^{\nu\mu})$ are the effective RIs of the core and cladding modes at the cladding mode resonant wavelength $\lambda_{\text{clad},m}^{\nu\mu}$. In the experiment, an optical spectrum analyzer (OSA, AQ6370B, Yokogawa) with the resolution of 0.02 nm and a supercontinuum spectrum light source (Superk Compact, NKT Photonics) will be adopted for the characterization of the spectrum.

3. Results and Discussions

3.1 Spectral Characteristics

In order to make it easier to analyze, the characteristic spectra of HO-TFBGs written with the pulse energy of 0.45 mJ/pulse and 0.60 mJ/pulse are shown in Fig. 2(a) and (c), respectively. The diffractive light spots achieved after the phase mask are shown in Fig. 2(b) and (d), which are captured by the camera. The zero order diffractive light spot with high pulse energy is obvious, which is beneficial for the formation of superposed RI modulation. It needs to declare that the diffractive

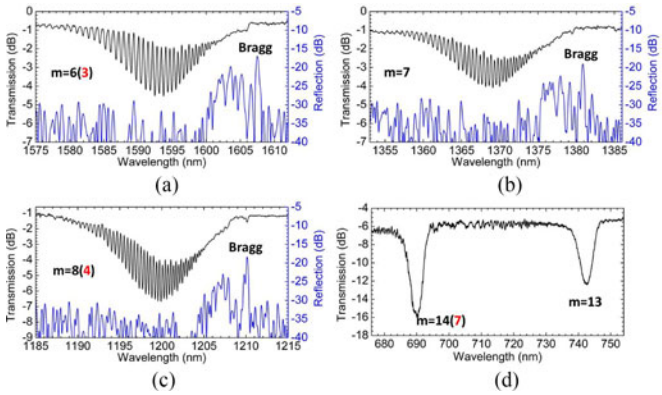

Fig. 3. The characteristics of the cladding mode resonances sets corresponding to (a) $m = 6(3)$, (b) $m = 7$, (c) $m = 8(4)$, and (d) $m = 13$ and 14(7) order Bragg diffractions.

light spot is tilted visually due to the pattern is captured in overlooking angle, which are parallel in reality. In the wide spectral range of 600–1700 nm shown in Fig. 2(c), two kinds of characteristic spectra are observed as expected, one kind corresponds to the major grating structures, i.e., the cladding mode resonances sets corresponding to the $m = (3)$–(7) order Bragg diffractions shown in the bracket; the other kind corresponds to the additional gratings, i.e., the characteristic spectra of $m = 6$–15 order gratings. These two kinds of spectra are superposed partially, and the resonance strength of the latter is weaker than the former. This kind of densely distributed high-order resonance spectrum is barely observed in Fig. 2(a), which only presents the high-order spectrum of the HO-TFBG written by pure ± 1 order beams interference. The transmission loss, which is obviously larger at the short wavelength region than that at the long wavelength region, is due to the Mie scattering caused by the RI change induced by the fs laser [16].

The close-up of the distribution of the 3 groups of cladding mode resonances sets above the cut-off wavelength in Fig. 2(c) is shown in Fig. 3(a)–(c). Bragg resonance exists obviously in the reflection spectrum, and typical cladding mode resonances frequency comb can be observed at the short wavelength side. However, in the wavelength range under the cut-off wavelength, there exist multiple modes. Due to the effective RI of each transmitting modes is close, the cladding mode resonances would be superposed. The cladding mode resonances sets shown in this waveband would be evolved into smooth loss envelop, and an example is given in Fig. 3(d).

3.2 Sensing Characteristics

For the study of the sensing characteristics of the fs-written HO-TFBG, the focus is the same order cladding mode resonances in each cladding mode resonances sets. RI measurement based on the cladding mode resonances is the typical function of TFBG. To study the surrounding RI sensing characteristic, the sensor was immersed into glycerol-water mixture solution with RI range of 1.3317∼1.4484. The *m*-LP021 cladding mode resonance was selected to monitor its RI response. For $m = 6(3)$, 7 and 8(4), the resonant wavelengths $\lambda^{021}_{\text{clad},m}$ were 1592.4895 nm, 1367.1973 nm, and 1198.4680 nm, respectively. We obtained the results of resonant wavelength shifts $\Delta\lambda^{021}_{\text{clad},m}$ that changed with RI, as shown in Fig. 4. The inset showed the response of 8(4)-LP021 cladding mode resonance to surrounding RI, and the spectra were vertically offset from each other for a better illustration. In the linear RI response range of 1.3317∼1.4022, their sensitivities were 1.619, 1.401, and 1.075 nm/RI unit (RIU), the corresponding linearities of which were 0.988, 0.990 and 0.979, respectively. When RI increased to the value, at which the cladding mode was cut-off, the RI sensitivities reached the maximum, namely 33.710, 20.996, and 16.621 nm/RIU, respectively. The Bragg resonance, as is well known, is insensitive to surrounding RI. For the cladding mode resonances with the same mode order, the RI sensitivity decreased with the increase of Bragg

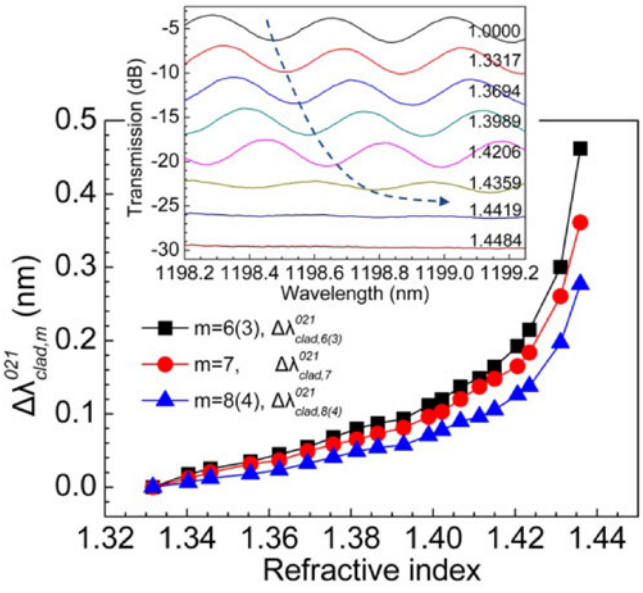

Fig. 4. Relationships between $\Delta\lambda^{021}_{\text{clad},m}$ and surrounding RI, the inset shows the spectrum shifts of 8(4)-LP021 cladding mode resonance versus the surrounding RI.

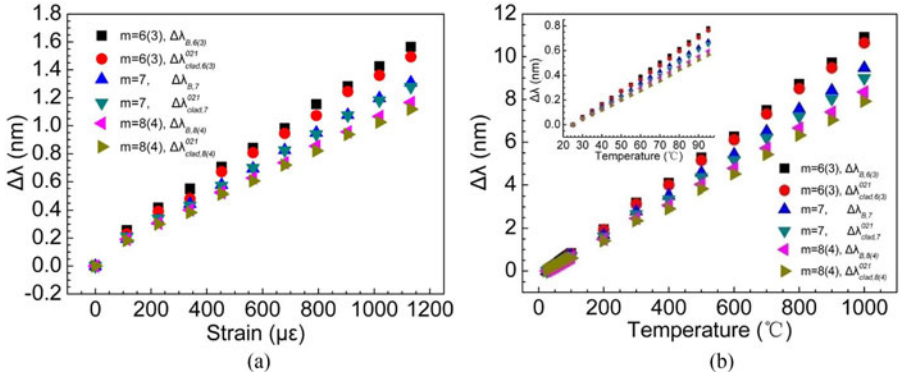

Fig. 5. (a) Relationships between $(\Delta\lambda^{021}_{\text{clad},m},\ \Delta\lambda_{B,m})$ and axial strain. (b) Relationships between $(\Delta\lambda^{021}_{\text{clad},m},\ \Delta\lambda_{B,m})$ and environment temperature. Inset: wavelength shifts change with temperature from room temperature to 100 °C.

diffraction order. This relationship could also be obtained according to the phase matching condition of cladding mode resonances.

In addition to the surrounding RI measurement, axial strain and temperature sensing of the fs-written HO-TFBG were also carried out. The study was realized by applying axial stress (0∼1.0 N) and increasing temperature (room temperature to 1000 °C). The axial strain applied on the fiber was calculated by equation $\varepsilon = F/\pi r^2 E$, where F was the axial stress, r was the cladding radius and E was the silica Young's modulus. Here, the responses of $\lambda^{021}_{\text{clad},m}$ to strain and temperature were analyzed. The sensing performance of Bragg resonance $\lambda_{B,m}$ of each order was tested to demonstrate that the sensitivity of Bragg resonance of the same order was similar to that of cladding mode resonances. $(\Delta\lambda^{021}_{\text{clad},m},\ \Delta\lambda_{B,m})$ variation changing with strain was exhibited in Fig. 5(a). Through the linear fitting, the strain sensitivities were calculated to be $(1.29,\ 1.33)_{6(3)}$, $(1.10,\ 1.13)_{7}$ and $(0.96,\ 1.00)_{8(4)}$ pm/$\mu\varepsilon$, respectively. The temperature influence on $(\Delta\lambda^{021}_{\text{clad},m},\ \Delta\lambda_{B,m})$ was also

linear fitted to be $(10.83,\ 11.11)_{6(3)}$, $(9.18,\ 9.62)_7$ and $(8.04,\ 8.47)_{8(4)}$ pm/°C, as shown in Fig. 5(b), among which, the inset showed a close-up illustration of the response from room temperature to 100 °C. The response sensitivities of $\lambda^{021}_{\text{clad},m}$ and $\lambda_{B,m}$ to strain or temperature were very close. However, the sensitivity differences between $\lambda^{021}_{\text{clad},m}$ and $\lambda^{021}_{clad,m\pm1}$, as well as the differences between each order Bragg resonance, were large. The above high temperature sensing up to 1000 °C is the advantage of fs-written TFBG. However, if it works at high temperature for long time, due to the softening and surface damage of silica fiber, it would affect the stability and mechanic performance of the sensor seriously. However, this kind of sensor could be competent for the normal bio-chemical sensing environment under 100 °C.

Furthermore, as can be predicted, in the fabrication process of fs-written HO-TFBG, if we use higher order phase mask or increase the grating tilting angle, the connection between adjacent cladding mode resonances sets can be realized, even the partial superposition. This may be able to increase the linear response range of RI measurement. For sensing applications of multiplexing TFBG, the presented three groups of high-order resonance frequency bands above cut-off wavelength are obvious insufficient. The ways to increase measurement frequency band, apart from utilizing higher-order phase mask to form denser high-order resonances, we can also choose special fiber with low cut-off wavelength or use the resonance sets above 1600 nm.

4. Conclusion

In conclusion, we demonstrated a fs-written HO-TFBG sensor with the superposed RI modulation. The superposed grating structure was realized by exposing the tilted fiber to the "twin pulses", which consisted of the ±1 order diffractive pulses and zero order pulses, with the time interval less than the lattice thermal diffusing time in the diffraction order walk-off area of the high-order phase mask. The fs-written HO-TFBG shows two kinds of high-order Bragg resonance and cladding mode resonances sets in wide spectral range, which correspond to the fringe periods of the ±1 order pulses interference light field and zero order pulse light field, respectively. The sensing characteristics of each order cladding mode resonances to surrounding RI, axial strain and temperature are also validated. Moreover, the multi-waveband frequency comb characteristic of the fs-written HO-TFBG may be used as novel fiber filter applied in the area of optical communication.

References

[1] T. Erdogan and J. E. Sipe, "Tilted fiber phase gratings," *J. Opt. Soc. Amer. A*, vol. 13, no. 2, pp. 296–313, Feb. 1996.
[2] J. Albert, L. Y. Shao, and C. Caucheteur, "Tilted fiber Bragg grating sensors," *Laser Photon. Rev.*, vol. 7, no. 1, pp. 83–108, Jan. 2013.
[3] T. Guo, F. Liu, B. O. Guan, and J. Albert, "Tilted fiber grating mechanical and biochemical sensors," *Opt. Laser Technol.*, vol. 78, pp. 19–33, Apr. 2016.
[4] G. Laffont and P. Ferdinand, "Tilted short-period fibre-Bragg-grating-induced coupling to cladding modes for accurate refractometry," *Meas. Sci. Technol.*, vol. 12, no. 7, pp. 765–770, Jul. 2001.
[5] B. Luo, Z. Yan, Z. Sun, Y. Liu, M. Zhao, and L. Zhang, "Biosensor based on excessively tilted fiber grating in thin-cladding optical fiber for sensitive and selective detection of low glucose concentration," *Opt. Exp.*, vol. 23, no. 25, pp. 32429–32440, Dec. 2015.
[6] T. Guo, "Fiber grating-assisted surface plasmon resonance for biochemical and electrochemical sensing," *J. Lightw. Technol.*, vol. 35, no. 16, pp. 3323–3333, Aug. 2017.
[7] J. Zheng *et al.*, "Magnetic field sensor using tilted fiber grating interacting with magnetic fluid," *Opt. Exp.*, vol. 21, no. 15, pp. 17863–17868, Jul. 2013.
[8] W. Lin *et al.*, "Two-dimensional magnetic field vector sensor based on tilted fiber Bragg grating and magnetic fluid," *J. Lightw. Technol.*, vol. 31, no. 15, pp. 2599–2605, Aug. 2013.
[9] M. D. Baiad and R. Kashyap, "Concatenation of surface plasmon resonance sensors in a single optical fiber using tilted fiber Bragg gratings," *Opt. Lett.*, vol. 40, no. 1, pp. 115–118, Jan. 2015.
[10] D. Feng, W. Zhou, X. Qiao, and J. Albert, "Compact optical fiber 3D shape sensor based on a pair of orthogonal tilted fiber Bragg gratings," *Sci. Rep.*, vol. 5, Nov. 2015, Art. no. 17415.
[11] W. X. Xie, M. Douay, P. Bernage, P. Niay, J. F. Bayon, and T. Georges, "Second order diffraction efficiency of Bragg gratings written within germanosilicate fibres," *Opt. Commun.*, vol. 101, nos. 1/2, pp. 85–91, Aug. 1993.
[12] C. M. Rollinson, S. A. Wade, B. P. Kouskousis, D. J. Kitcher, G. W. Baxter, and S. F. Collins, "Variations of the growth of harmonic reflections in fiber Bragg gratings fabricated using phase masks," *J. Opt. Soc. Amer. A*, vol. 29, no. 7, pp. 1259–1268, Jul. 2012.

[13] G. Statkiewicz-Barabach, K. Tarnowski, D. Kowal, P. Mergo, and W. Urbanczyk, "Fabrication of multiple Bragg gratings in microstructured polymer fibers using a phase mask with several diffraction orders," *Opt. Exp.*, vol. 21, no. 7, pp. 8521–8534, Apr. 2013.
[14] S. J. Mihailov, D. Grobnic, C. W. Smelser, P. Lu, R. B. Walker, and H. Ding, "Induced Bragg gratings in optical fibers and waveguides using an ultrafast infrared laser and a phase mask," *Laser Chem.*, vol. 2008, 2008, Art. no. 416251.
[15] M. Bernier, S. Gagnon, and R. Vallée, "Role of the 1D optical filamentation process in the writing of first order fiber Bragg gratings with femtosecond pulses at 800 nm," *Opt. Mater. Exp.*, vol. 1, no. 5, pp. 832–844, Sep. 2011.
[16] J. Thomas, C. Voigtländer, R. Becker, D. Richter, A. Tünnermann, and S. Nolte, "Femtosecond pulse written fiber gratings: A new avenue to integrated fiber technology," *Laser Photon. Rev.*, vol. 6, no. 6, pp. 709–723, Nov. 2012.
[17] C. Chen *et al.*, "Reflective optical fiber sensors based on tilted fiber Bragg gratings fabricated with femtosecond laser," *J. Lightw. Technol.*, vol. 31, no. 3, pp. 455–460, Feb. 2013.
[18] J. D. Mills, C. W. J. Hillman, B. H. Blott, and W. S. Brocklesby, "Imaging of free-space interference patterns used to manufacture fiber Bragg gratings," *Appl. Opt.*, vol. 39, no. 33, pp. 6128–6135, Nov. 2000.
[19] S. A. Wade, W. G. A. Brown, H. K. Bal, F. Sidiroglou, G. W. Baxter, and S. F. Collins, "Effect of phase mask alignment on fiber Bragg grating spectra at harmonics of the Bragg wavelength," *J. Opt. Soc. Amer. A*, vol. 29, no. 8, pp. 1597–1605, Aug. 2012.
[20] D. Grobnic, S. J. Mihailov, C. W. Smelser, and R. B. Walker, "Multiparameter sensor based on single high-order fiber Bragg grating made with IR-femtosecond radiation in single-mode fibers," *IEEE Sens. J.*, vol. 8, no. 7, pp. 1223–1228, Jul. 2008.
[21] C. W. Smelser *et al.*, "Multiple-beam interference patterns in optical fiber generated with ultrafast pulses and a phase mask," *Opt. Lett.*, vol. 29, no. 13, pp. 1458–1460, Jul. 2004.
[22] S. J. Mihailov *et al.*, "UV-induced polarisation-dependent loss (PDL) in tilted fibre Bragg gratings: Application of a PDL equaliser," *Proc. IEE, Optoelectron.*, vol. 149, no. 5, pp. 211–216, Oct. 2002.
[23] C. W. Smelser, D. Grobnic, and S. J. Mihailov, "Generation of pure two-beam interference grating structures in an optical fiber with a femtosecond infrared source and a phase mask," *Opt. Lett.*, vol. 29, no. 15, pp. 1730–1732, Aug. 2004.
[24] J. Thomas *et al.*, "Inscription of fiber Bragg gratings with femtosecond pulses using a phase mask scanning technique," *Appl. Phys. A.*, vol. 86, no. 2, pp. 153–157, Feb. 2007.
[25] C. B. Schaffer, A. Brodeur, and E. Mazur, "Laser-induced breakdown and damage in bulk transparent materials induced by tightly-focused femtosecond laser pulses," *Meas. Sci. Technol.*, vol. 12, no. 11, pp. 1784–1794, Nov. 2001.
[26] S. M. Eaton *et al.*, "Heat accumulation effects in femtosecond laser-written waveguides with variable repetition rate," *Opt. Exp.*, vol. 13, no. 12, pp. 4708–4716, Jun. 2005.
[27] R. R. Gattass and E. Mazur, "Femtosecond laser micromachining in transparent materials," *Nature Photon.*, vol. 2, pp. 219–225, Apr. 2008.
[28] M. Malinauskas *et al.*, "Ultrafast laser processing of materials: From science to industry," *Light Sci. Appl.*, vol. 5, Aug. 2016, Art. no. e16133.
[29] R. Yang, Y. S. Yu, C. Chen, Q. D. Chen, and H. B. Sun, "Rapid fabrication of microhole array structured optical fibers," *Opt. Lett.*, vol. 36, no. 19, pp. 3879–3881, Oct. 2011.
[30] C. W. Smelser, S. J. Mihailov, and D. Grobnic, "Hydrogen loading for fiber grating writing with a femtosecond laser and a phase mask," *Opt. Lett.*, vol. 29, no. 18, pp. 2127–2129, Sep. 2004.